Thermochimica Acta, 58 (1982) 271–288
Elsevier Scientific Publishing Company, Amsterdam—Printed in The Netherlands

THERMOGRAVIMETRY OF SELECTED AMERICAN AND AUSTRALIAN OIL SHALES IN INERT DYNAMIC ATMOSPHERES *

C.M. EARNEST
Perkin-Elmer Corporation, Norwalk, CT 06856 (U.S.A.)

(Received 25 March 1982)

ABSTRACT

The pyrolysis profile for the U.S. Geological Survey SGR-1 Green River shale specimen is reported using computerized TG and DTG techniques. The thermal behavior of this specimen in dynamic nitrogen atmosphere is compared with that of a retort composite (spent shale) specimen obtained from one of the current thermal retorting processes. The quantitative differences between these two specimens are discussed in terms of the thermal retorting of shales from the Western United States.

A carefully performed comparative study of the Australian Rundle, Glen Davis, and Alpha Deposits as well as the USGS-SGR-1 Green River specimen is also given here. Using the results of this study, the pyrolysis onset temperatures and temperatures at maximum pyrolysis rate were related to the type of organic maceral components of the shale specimens. These shales were also compared for total carbon, hydrogen, and nitrogen content by elemental analysis.

A drilled core specimen from Western Colorado of known oil yield versus depth of seam was used to correlate the DTG pyrolysis peak area to the Fisher assay oil yield assignments. A method of precise assignment of DTG peak areas which is often overlooked is also demonstrated.

INTRODUCTION

Oil shale is a sedimentary rock which contains both inorganic (mineral) and organic (kerogen and bitumen) components. The term "oil shale" may be considered a misnomer in that it contains no free oil in its natural state. The oil is derived from the kerogen containing rock by destructive distillation. Most forms of organic matter in oil shales belong to the exinite group of macerals. These are largely algal in origin (alginite) with lesser contribution from spores, pollen, and cuticle of higher land plants [1].

Oil shales are found on all continents and are known to exist in nearly

---

* Presented at the 33rd Annual Pittsburgh Conference on Analytical Chemistry and Applied Spectroscopy, Atlantic City, New Jersey, March, 1982, Paper No. 840.

0040-6031/82/0000–0000/$02.75

three dozen countries. The world's highest grade oil shales, although limited in amounts, are the Australian torbinite deposits. When compared on a world wide scale, the U.S. Green River shales have been described [2] as about average in grade. However, the thickness of the Green River deposit and consistency of grade make it the world's largest known deposit. As will be seen in the work presented here, both the inorganic mineral components and the level and nature of the organic components determine the thermal behavior of the oil shale as a whole. The mineral matter composition varies with the location of the deposit and may reflect the historic aqueous environment at the time of deposition. Also, significant differences occur in the nature of the alginite from various oil shales. Thus, thermal curves obtained from differential scanning calorimetry (DSC), differential thermal analysis (DTA), thermogravimetry (TG), and derivative thermogravimetry (DTG) may reflect these differences.

Due to the fact that thermal retorting is one of the most common approaches to the processing of oil shales, the thermal methods of analysis DSC, DTA, TG, and DTG are obvious choices for collecting data on the raw shale related to its behavior during retorting. These techniques have been applied to assign the energy of pyrolysis and activation energies [3] of several oil shale specimens. Non-isothermal kinetics have been performed by TG using kerogen concentrate [4] and in some seams where there were no interfering mineral components, the oil yield has been correlated to the pyrolysis energy by DSC [5]. Evolved gas analysis (EGA) and evolved gas detection (EGD) accomplished by interfacing numerous detection and/or analysis systems to the exit stream of pyrolysis vapor, offer additional approaches to the characterization of oil shales by thermal analysis techniques. Notable examples are the use of flame ionization detection in EGD [6] and GC–mass spectroscopy in EGA.

The recent addition of microcomputer control to thermal analysis instrumentation has led to improved temperature control and hence increased reproducibility of thermal curves obtained from thermal analysis techniques. Enhanced data acquisition and reduction have been accomplished through the use of minicomputers in conjunction with thermal analysis systems. One obvious advantage of the use of such computers when performing thermogravimetry of oil shales of unknown levels of organic and mineral components is that one would never have to repeat the analysis because of improper choice of ordinate sensitivity. The ordinate (percent weight loss) values may be rescaled to optimize the thermal curve for the purposes of both mass loss assignment and hard copy print-out. In some commercial instruments of this type, this rescaling is performed automatically on receipt of the data from the entire thermogravimetric experiment. Furthermore, the data may be stored on a data disk and recalled for analysis at a later date.

EXPERIMENTAL

Oil shale specimens used in this study

The Green River shale specimen used for the comparative study was the U.S. Geological Survey SGR-1 oil shale specimen. The Green River retort composite sample was obtained from one of the current thermal retorting processes. Another set of Green River specimens was obtained from a core drilled seam in Western Colorado in which the Fisher assay oil yield had been assigned versus depth of the seam.

The five Australian specimens included in this study were donated by the Australian Department of Defense Materials Research Laboratories in Marsbyrong, Victoria. These include three specimens from the Rundle

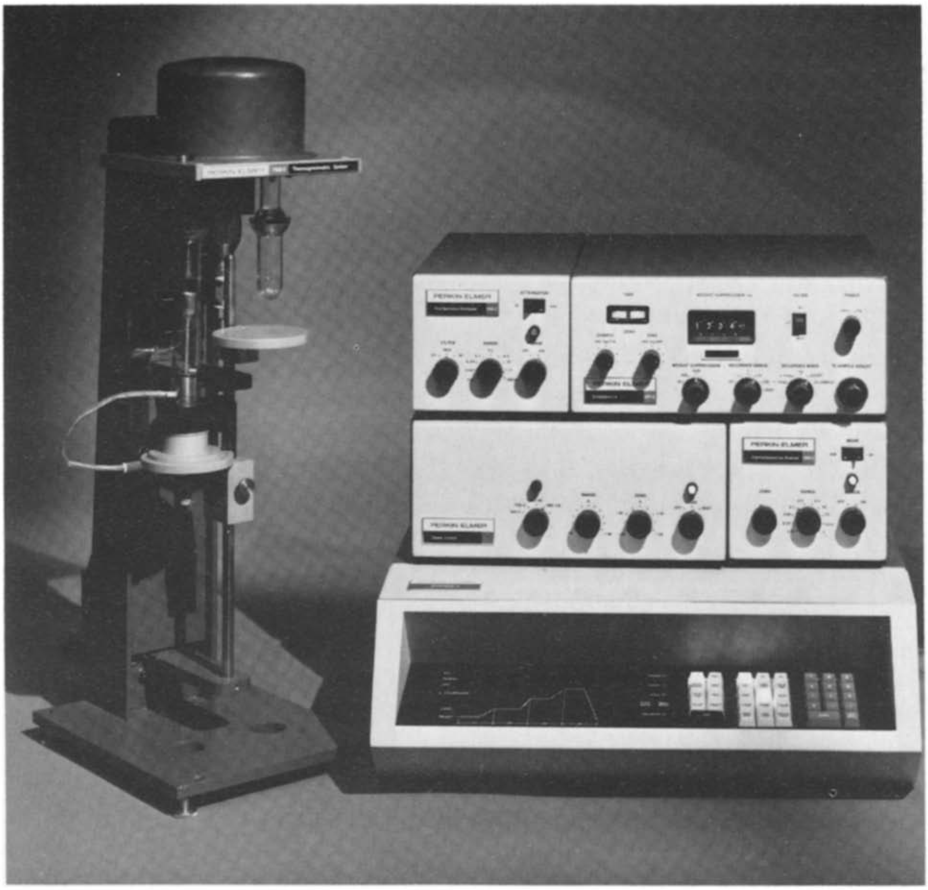

Fig. 1. Perkin-Elmer TGS-2 thermogravimetric analysis system with system 4 microcomputer controller.

deposit located near Gladstone, Queensland. This is probably the most important Australian deposit at the moment. A massive project is in the early stages which could lead to the processing of as much as 500,000 tonnes of Rundle shale per day. Two of the rich Australian torbanite deposits were also studied. One was obtained from the historic Glen Davis deposit located in the Sydney basin of New South Wales. This seam was mined and processed from approximately 1940 and ceased operations in 1952. The main seam reportedly [7] had a Fisher assay of 590 l tonne^{-1}. The other torbanite specimen was obtained from the Queensland Alpha deposit located on the eastern edge of the Galilee Basin.

Instrumental

All elemental analysis results given in this paper were obtained using the Perkin-Elmer model 240C elemental analyzer in conjunction with the model 240DS data station. All results of thermogravimetry were obtained with the Perkin-Elmer TGS-2 thermogravimetric analysis system used in conjunction with the system 4 microcomputer controller shown in Fig. 1. The data handling device used for the comparative studies of the USGS-SGR-1 Green River shale specimen with the Green River thermal retort composite was the Perkin-Elmer thermal analysis data station (TADS) shown in Fig. 2. All

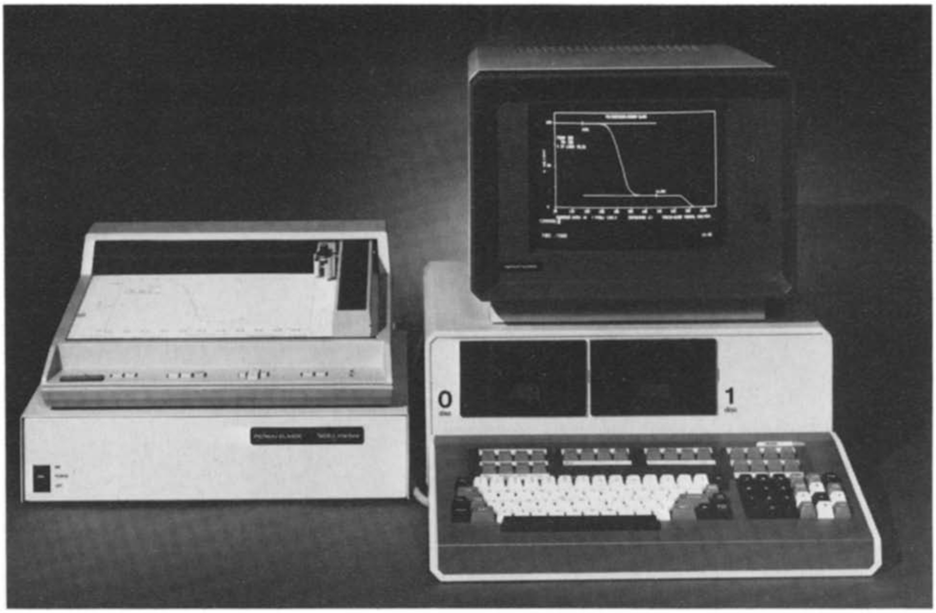

Fig. 2. Perkin-Elmer thermal analysis data station and printer-plotter.

other thermal curves were obtained using the Perkin-Elmer $X-Y_1Y_2$ thermal analysis recorder.

RESULTS AND DISCUSSION

Elemental analysis

The results obtained using the Perkin-Elmer model 240C elemental analyzer in the normal C, H, and N mode of operation are given in Table 1. As can be seen from these results, the Queensland Alpha deposit appears to be the richest deposit in terms of total carbon content (78.00%). This is followed by the other torbanite specimen, the Glen Davis deposit, with 54.83% total carbon. The Rundle and Green River specimens appear to be similar in organic carbon content when one considers the fact that the Green River specimen (as will be seen in the TG studies presented later) contains ca. 3.8% inorganic (carbonate) carbon. The Green River specimen contained much more carbonate mineral than did the Rundle shale specimens.

TG studies in inert dynamic atmospheres as related to thermal retorting of Green River shales

Figure 3 shows the results obtained when a 30.63 mg sample of the USGS-SGR-1 Green River shale specimen is heated at 10°C $\min^{-1}$ using a dynamic purge of dry nitrogen of 70 $cm^3 \min^{-1}$ using the TGS-2 thermogravimetric analysis system, system 4 microcomputer controller, and thermal analysis data system (TADS). The solid line represents the initial TG thermal curve as displayed by the TADS CRT screen after automatic

TABLE 1

Elemental analysis of Australian and Green River (SGR-1) oil shale specimens

Specimen		C (%)	H (%)	N (%)
Rundle	Drum 5556	25.14	3.90	0.40
	RAH-65	26.33	3.24	0.64
	Lot 6001	18.89	2.84	0.56
Glen Davis		54.83	6.92	0.85
Alpha deposit		78.00	10.50	0.96
Green River (SGR-1)		28.02	3.05	0.88

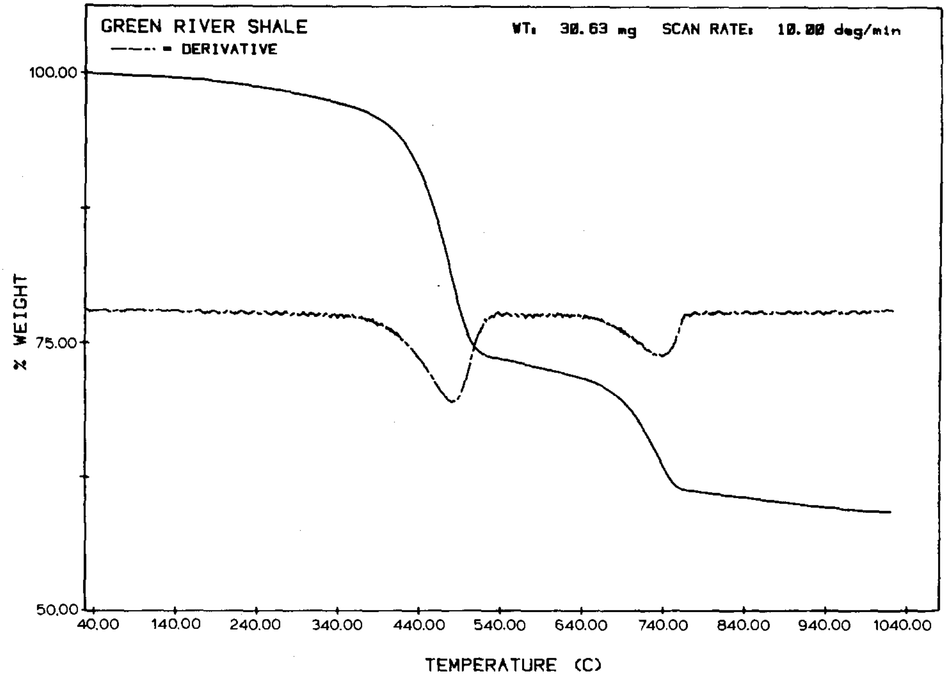

Fig. 3. TG and DTG thermal curves for USGS-SGR-1 oil shale specimen.

rescaling of the ordinate data from 100 to 50% of the initial sample weight. The derivative thermogravimetric (DTG) thermal curve described by the dotted line was obtained after the TG data had been displayed by the TADS. The derivative trace was then generated via the basic program incorporated into the TADS TG standard software. Both TG and DTG thermal curves may be further rescaled by simple key strokes on the TADS keyboard.

It has been the experience of the author that the two stage mass loss profile described in Fig. 3 is typical for most shales from the upper and mahogany zones of the Green River formation. Notable exceptions to this would be those shales containing significant amounts of trona, dawsonite, nahcolite, pyrite, and marcasite which are discussed later in this paper. In the thermal curves presented in Fig. 3, the initial decomposition in the 300–550°C temperature range is due to the major organic (kerogen plus bitumen) pyrolysis event while the thermal event observed at higher temperatures is due primarily to the evolution of carbon dioxide from the decomposition of the carbonate mineral component(s) of the shale specimen. The magnitude of these mass loss events will vary with the level of organic and carbonate mineral components. Although the carbonate components may be calcitic, dolomitic, or ankeritic, these are not easily distinguished in dynamic nitrogen atmospheres by TG.

This mass loss profile obtained in inert dynamic atmosphere is of particular interest since it is related to the behavior of the oil shale specimen during thermal retorting. It is easy to see from this TG thermal curve why such thermal retorting processes are carried out at or near 500°C since the endothermic carbonate decomposition would reduce the retorting efficiency in terms of oil yield per unit energy required for the retorting process. One will also note the continuous 'bleed' of the specimen on heating to higher temperatures.

There are two factors which contribute to this continued weight loss. First, is the possibility of continued pyrolysis in and beyond the carbonate decomposition region which is supported by TG–FID studies [6]. Second, the CO_2 evolved from the carbonate decomposition is known to react with the residual char

$$C(char) + CO_2(g) \rightarrow 2\,CO(g)$$

forming carbon monoxide gas [11]. The net effect of this reaction is a continued mass loss and reduction in the amount of residual organic carbon in the char. Mallon and Braun [11,14] have performed a theoretical treatment of the rate of this reaction in large 8 kg bricks of Green River shales

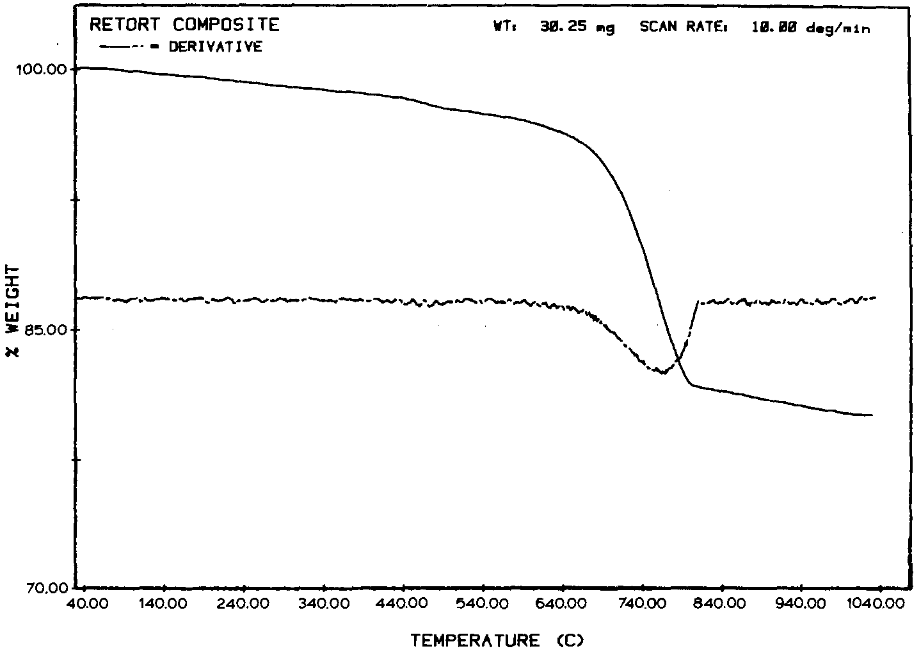

Fig. 4. TG and DTG thermal curves for a Green River retort composite.

using the basic assumptions of first-order dependence on both the char concentration in the core of the brick and P_{CO_2}. In thermogravimetry, the observation of this reaction in dynamic nitrogen atmosphere will be governed to a large extent by the total mass of carbonate in the shale sample, which directly relates to the initial P_{CO_2} achieved above the pyrolyzed residue. In dynamic nitrogen purge, this initial P_{CO_2} will diminish with time as the CO_2 is swept from the TG furnace tube. Thus, the factors which affect the extent of this reaction in a thermogravimetric apparatus in dynamic nitrogen atmospheres are sample size, percentage carbonate in the sample, volume of the TG furnace tube, flow rate of the nitrogen purge, entropy of mixing of purge and product gases, and the amount of char in the pyrolyzed residue.

The large amounts of spent shale residues obtained as a by-product from the thermal retorting processes must be disposed of or used for some other industrial purpose. Some suggested uses [1] include raw materials for the cement and building industries or as possible soil conditioners. This, of course, will depend upon the composition of the spent shales. A certain amount of the original organic content of the shales remains in the spent shale as thermally altered kerogen and as fixed carbon residue. Figure 4 shows the TG and DTG thermal curves obtained from the TGS-2/TADS system for an actual retort composite specimen. The diminished level of organic pyrolysis in the 300–500°C temperature interval and an increase in the level of carbonate mineral component is obvious from this thermal curve. Table 2 lists the percent mass loss assignments for the two temperature ranges of interest as assigned by the TADS. Such comparisons of raw Green River specimens by thermogravimetry both before and after thermal retorting can lend valuable information in terms of the removal of the organic matter. As one can see in the table, the retort composite sample loses only 3.01% of the original sample weight on heating to 550°C versus 26.57% in the SGR-1 Green River specimen.

There have been several additional factors reported which relate to the

TABLE 2

Comparative TG mass loss assignment for Green River shale SGR-1 specimen and Green River retort composite

Specimen	Mass loss (%)		
	30–550°C	550–850°C	30–1025°C
Green River shale (SGR-1)	26.57	15.51	40.20
Green River retort composite	3.01	14.43	20.19

carbonate decomposition region of Green River shales. The first is the previously mentioned reaction of carbon dioxide with the organic carbon of the residual char [11]. Second, experiments with heated blocks of Green River shale specimens [11] have exhibited retention of part of the carbon dioxide due to the formation of non-stoichiometric amounts of spurrite, $Ca_5Si_2O_8CO_3$. Third, is the possible reaction of the metal oxide decomposition products of calcite and dolomite with quartz [12,13]. The latter would have no effect on TG results, however.

Despite these possibilities of variable and uncertain magnitude, the comparative TG results of this study show that the retort composite sample loses 1.08% more by weight in the carbonate decomposition region than the SGR-1 Green River shale. This increase of the carbonate mineral component is better shown when the mass losses in the 550–850°C temperature interval are expressed as a percentage of the total mass loss of each specimen. When this is done, 71.47% of the total mass loss in the retort composite specimen occurs between 550 and 850°C while the SGR-1 shale specimen loses only 38.58% of its total mass loss in the same temperature region. This becomes more obvious in Fig. 4 where both TG thermal curves are displayed simultaneously by the TADS.

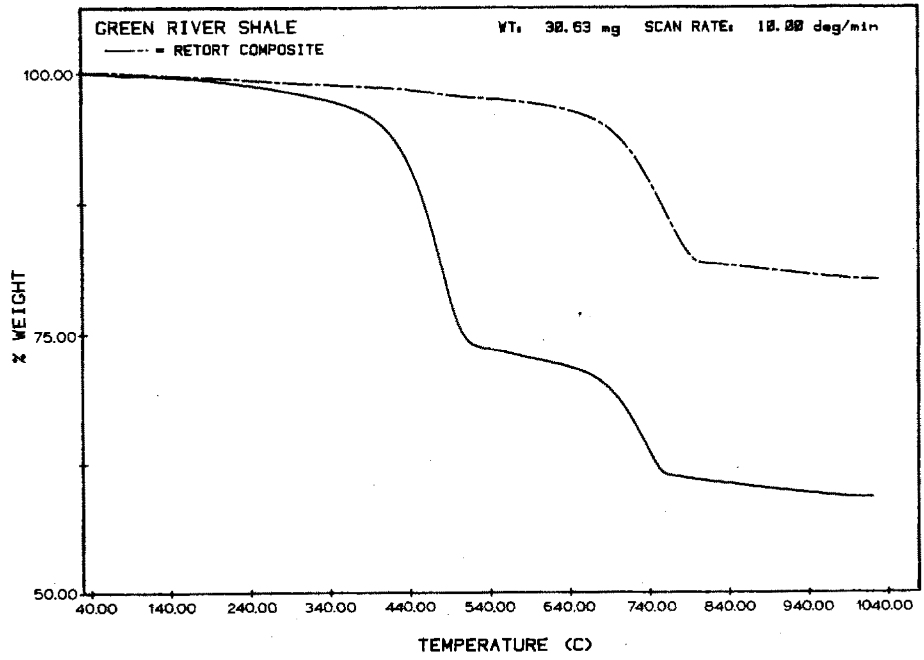

Fig. 5. Simultaneous display of TG thermal curves for SGR-1 Green River shale and Green River retort composite.

As was mentioned earlier, this concentration of the carbonate mineral component in Green River spent shales is both expected and necessary from an economic standpoint in the processing of these oil shales. On the other hand, the effective use of the residual organic carbon in spent shales as a fuel source is lessened due to the cooling effect (endothermic) which the large carbonate component would exhibit at combustion temperatures. It should again be stated that evolved CO_2 from the carbonate component of these shales contributes another endothermic effect by reacting with the residual char to produce carbon monoxide. However, in combustion atmospheres, the carbon monoxide thus formed then reacts with available oxygen exothermically liberating additional heat for the retorting process [11].

Comparative results of pyrolysis profiles of Australian and Green River shale specimens by TG

The five Australian specimens as well as the SGR-1 Green River shale were subjected to a comparative examination using the TGS-2 thermogravimetric analysis system, system 4 microcomputer controller, and Perkin-Elmer X–Y_1Y_2 recorder. In this case, the DTG thermal curve was obtained using the Perkin-Elmer Model FDC-1 first derivative computer which is standard with the TGS-2 thermogravimetric system. The temperature axis was calibrated using Curie point standards nickel, perkalloy, and iron for this study.

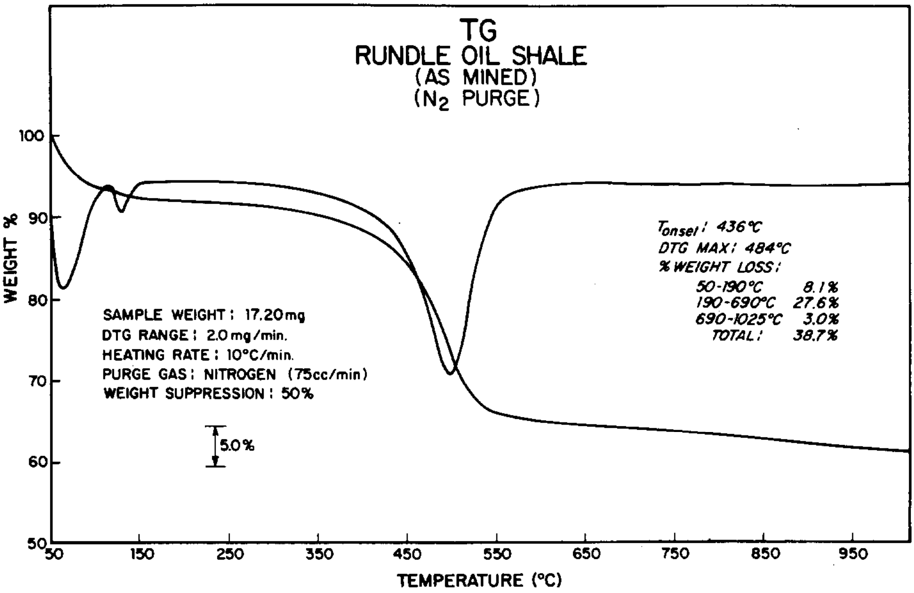

Fig. 6. TG and DTG thermal curves for Rundle Drum 5556 (as mined) shale specimen.

Samples of similar weight were heated at 10°C min^{-1} under a dynamic purge of dry nitrogen at 75 cm^3 min^{-1}.

Figure 6 shows the TG and DTG thermal curve for the Drum 5556 Rundle shale specimen. This raw shale (as mined) specimen was reported by the mine company to be typical and gave a Fisher assay of 114 l $tonne^{-1}$ of raw shale and a water content from the collected distillate of 28.7%. One will note that the major difference between this mass loss profile and that of the Green River shale is the presence of low temperature peaks (possibly loss of water from clay mineral components) and the absence of major quantities of carbonate decomposition at higher temperatures.

The results of the entire comparative study are given in Table 3. The RAH-65 Rundle specimen was selected from a dried one ton lot and this is reflected by the absence of one of the peaks in the 100–150°C temperature region (Fig. 7) and also by the tabulated total weight loss to 190°C. The other Rundle specimen (Lot 6001) is a lower grade shale as was indicated by the elemental analyses given earlier as well as the mass loss profile presented in Fig. 8.

Although much less than that observed in the Green River specimen, all three Rundle specimens showed measurable carbonate component in the TG–DTG thermal curves. Using the DTG curve as the indicator for the beginning and the end of the CO_2 evolution, the percentage mass loss due to carbonate decomposition was assigned for each. These values were then multiplied by the stoichiometric factor CO_3^{2-}/CO_2 or 1.36. The resulting carbonate contents expressed as % CO_3^{2-} for the Drum 5556, Lot 6001, and RAH 65 specimens were 2.31, 1.56, and 4.42%, respectively. No measurable carbonate was observed for the Glen Davis and Alpha torbinite specimens (Figs. 9 and 10).

TABLE 3

Comparative pyrolysis study of Australian and Green River shale specimens by TG and DTG

Specimen		Weight loss (%)			Pyrolysis temp. (°C)	
		190°C	690°C	1025°C	T_{onset}	DTG max
Rundle	Drum 5556	8.1	35.7	38.7	436	484
	RAH-65	5.7	32.2	36.1	412	472
	Lot 6001	4.1	26.4	28.9	422	478
Alpha deposit		0.7	86.2	87.2	469	498
Glen Davis deposit		1.0	54.2	55.0	482	504
Green River shale		1.8	28.0 *	40.2	429	479

* Value taken at 630°C due to carbonate decomposition.

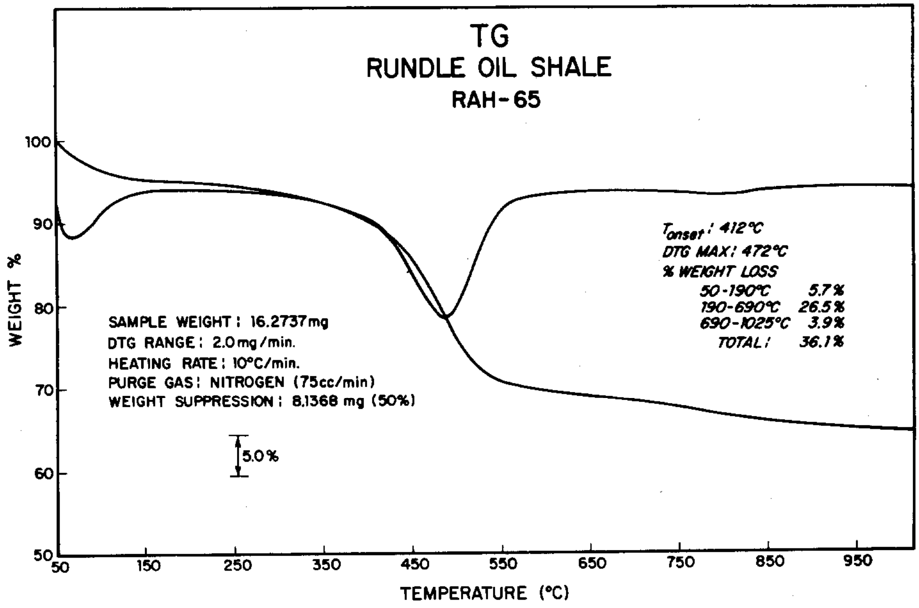

Fig. 7. TG and DTG thermal curves for Rundle RAH-65 shale specimen.

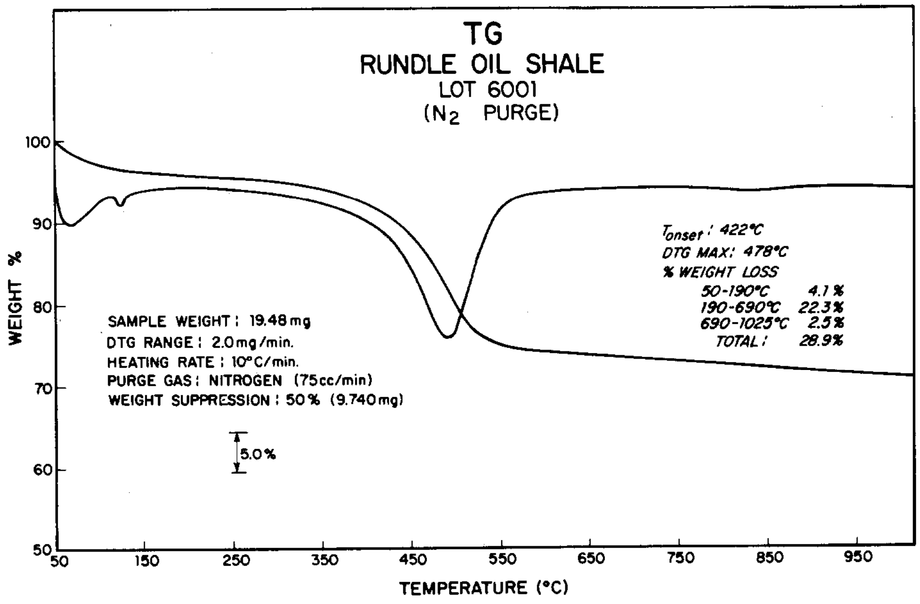

Fig. 8. TG and DTG thermal curves for Rundle Lot 6001 shale specimen.

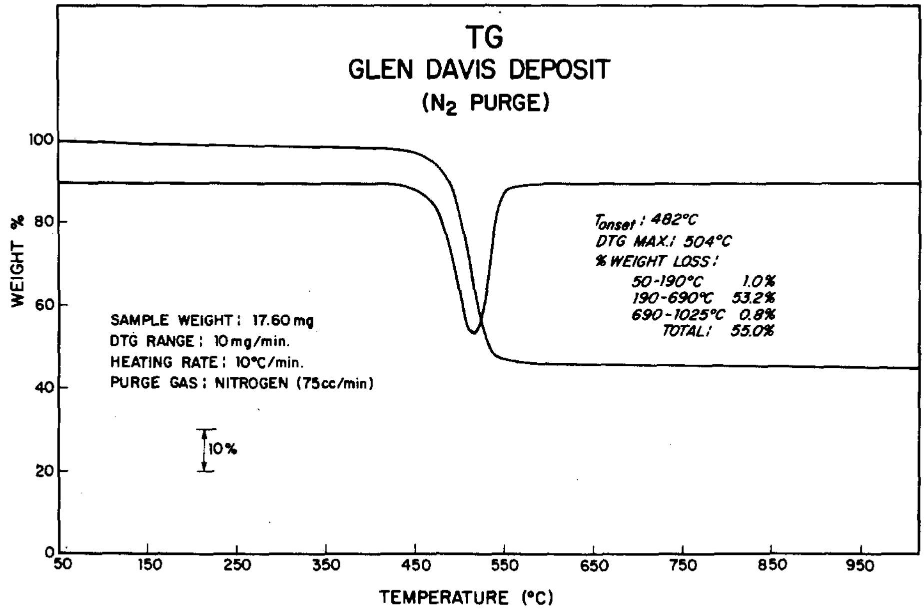

Fig. 9. TG and DTG thermal curves for Glen Davis shale specimen.

The Rundle shales typically contain abundant pyrite (FeS_2). This is not evidenced by the TG or DTG thermal curves in inert atmospheres because the decomposition of the pyrite to pyrhotite ($Fe_{1-x}S$) occurs within the temperature interval as the major kerogen pyrolysis event. The total sulfur content of the Drum 5556 (as mined) specimen was determined to be 1.25% using the model 240C elemental analyzer in the sulfur analysis mode. This would indicate a maximum pyrite concentration of 2.34% for this raw shale specimen.

Before proceeding with the TG–DTG comparative studies, some of the microscopy studies of Dr. Allan Cook and his co-workers [1] relating to these shales should be cited. In these studies conducted at the University of Wollongong in New South Wales, both the Rundle and Green River algal components were classified as Alginite B and originated from an historic blue-green algae (*Cyanophyceae*). The organic matter in the Australian Rundle and U.S. Green River shales bear a striking resemblance and in each comprises almost entirely lamellar alginite with minor amounts of corpohuminite. By comparing both the extrapolated onset temperatures and the DTG peak maxima given in Table 3, one can see that the Rundle and Green River specimens are quite similar, both in thermal stability and temperature of maximum pyrolysis rate when compared with the other specimens in this study.

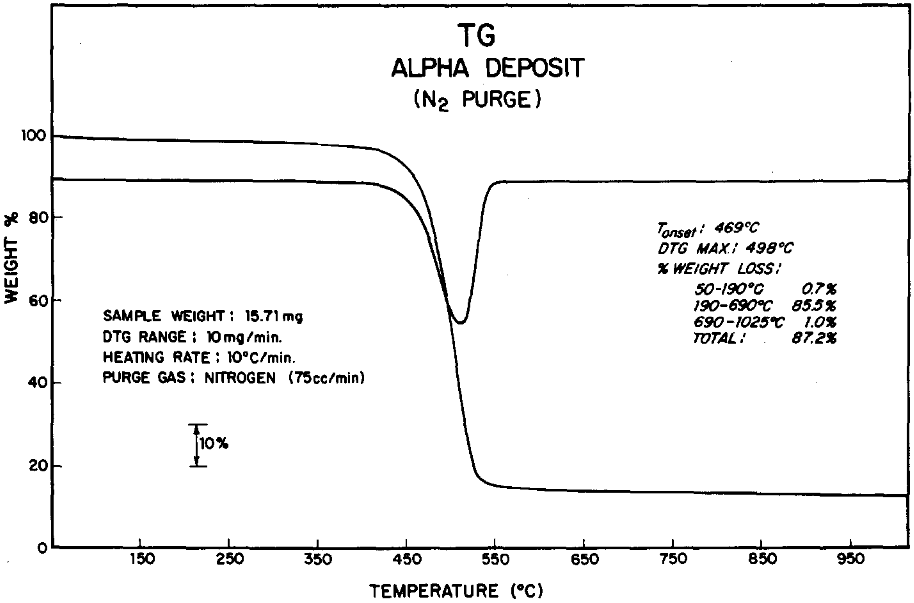

Fig. 10. TG and DTG thermal curves for Alpha deposit shale specimen.

On the other hand, the torbanite deposits (Glen Davis and Alpha) both contain a different type of Alginite (Alginite A) from that found in the Green River and Rundle shales. According to Cook et al. [1], Alginite A originates from historic green algae. Both the Glen Davis and Alpha deposits contain minor amounts of vitrinite, inertite, and sporinite as non-algal maceral components. Again, the extrapolated onset temperatures and DTG peak maxima obtained in this study indicate a similarity in the major pyrolysis peaks for these two torbanite specimens. It was also found that a similar correlation is observed in the oxidative profiles of these shales by thermal analysis using dynamic air atmospheres. These results will be presented as a portion of a future publication to appear in this journal [10].

Variation of oil yield with depth of seam for a Green River core specimen

The variation of oil yield with depth of seam is a valuable assignment from the economic standpoint for both exploration assignments and subsequent process expectations. All oil yield assignments for oil shales are determined by the Fisher assay method [8] or some modified form thereof [9]. As mentioned earlier, in the absence of significant amounts of certain interfering minerals, the oil yield of some Green River shales has been correlated to the energy assignment of the major pyrolysis endothermic peak obtained by 'heat flux' DSC [5].

Since thermogravimetry has historically been considered more quantitative than 'heat flux' DSC, and the fact that the same pyrolysis event is observed by TG and DTG, a similar study was undertaken in our laboratories.

First, an examination of the minerals commonly found in the Green River shales were studied by both TG, DTG, and DTA. It was observed that trona ($NaHCO_3 \cdot Na_2CO_3 \cdot 2\,H_2O$) and nahcolite ($NaHCO_3$) decomposed at temperatures below the major kerogen decomposition onset, and did not interfere, while dawsonite ($NaAl[OH]_2CO_3$), pyrite (FeS_2), marcasite (FeS_2) and siderite ($FeCO_3$) would interfere with the DTG peak area measurement. No specimen of analcite ($NaAlSi_2O_6 \cdot H_2O$) was available for study but has been listed by Rajeshwar [5] as a possibly interfering mineral specie. Quartz is not observed at all by thermogravimetry and clay minerals are minor components of the Green River shales.

Six oil shale specimens from the same seam at depths varying from 50 to 115 m were subjected to simultaneous TG–DTG analysis using the TGS-2 thermogravimetric analysis system. The samples were ground prior to analysis to pass a −200 mesh screen. The oil yield values were assigned external to our laboratory and ranged from 44.6 to 282.7 l tonne^{-1}. A heating rate of 10°C min^{-1} and a dynamic purge of 70 cm^3 min^{-1} of dry nitrogen were employed. All experiments were carried out in triplicate with the exception of the 124.7 l tonne^{-1} sample which was chosen for our extended precision study. This specimen was run five times.

Figure 11 shows a rapid method of assignment of DTG peak areas in any thermogravimetric study. Since the TG thermal curve represents the integral of the DTG trace between any two temperatures of simultaneous measurement, the DTG peak area may be determined in percentage mass loss by reading the ordinate value of the TG curve at the temperature of initiation, T_a, of the DTG peak and again when the DTG curve returns to constant rate (T_b). In practice, the precision of this method is very good and is enhanced by microcomputer control of the instrument, microbalance reproducibility, and sample homogeneity. It is particularly applicable to the study of Green River shales since a continuous 'bleed' or mass loss, at essentially constant rate, is observed in inert purge atmospheres before the temperature of initiation and after the return of the DTG curve to constant rate for the major kerogen decomposition peak.

Table 4 shows the results obtained for the six oil shale core samples. In this study, the average deviation for the assignment of the DTG pyrolysis peak area was 0.1% at all oil yield levels. The relative standard deviation varied from 1.4% for the 44.6 l tonne^{-1} sample to 0.45% for the 283 l tonne^{-1} specimen.

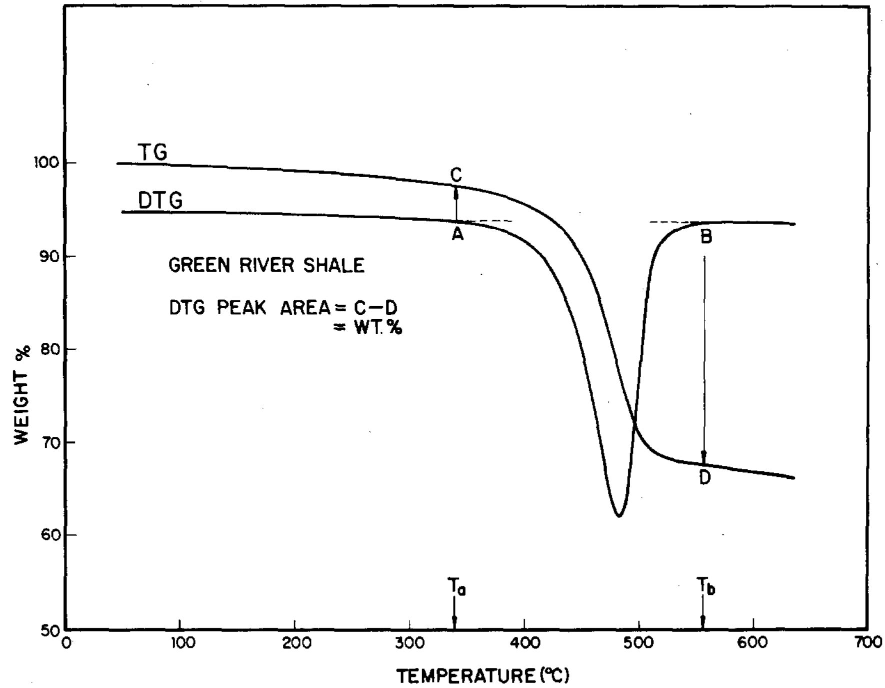

Fig. 11. Assignment of DTG peak area from TG thermal curve.

Figure 12 shows the linear correlation of the DTG pyrolysis peak area with the known Fisher assay values for the Green River oil shales studied here. It is important to note that the plot extrapolates to within experimental error of zero oil yield for zero peak area. This implies that, for this set of samples, the contribution to the DTG peak area by interfering minerals was very minor. The method of least squares was employed to determine the

TABLE 4

Correlation of DTG peak area with oil yield for Green River shales

Oil yield (l Tonne^{-1})	DTG peak area (wt.%)
44.6	4.9
83.4	9.1
124.7	13.9
170.1	19.2
208.9	24.0
282.7	31.9

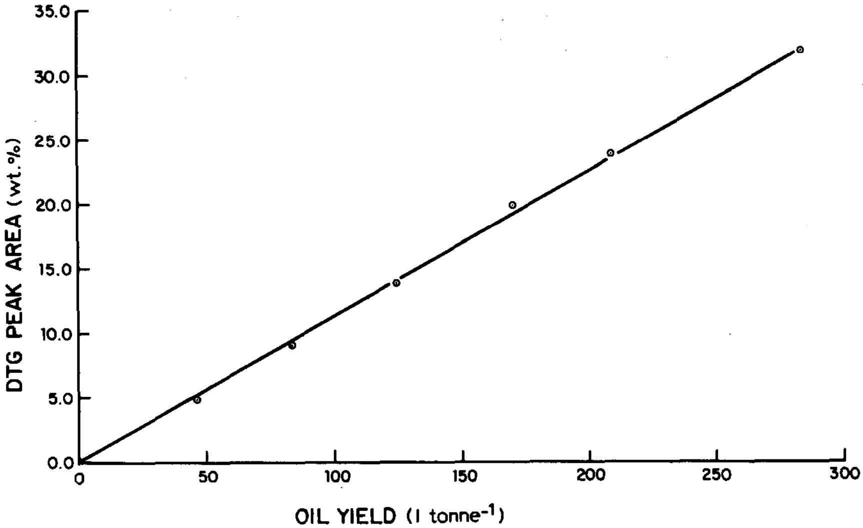

Fig. 12. Linear correlation of DTG pyrolysis peak area with Fisher assay oil yield values.

coefficient of linear regression for this plot. The resulting relationship obtained is

$$\text{DTG area (wt.\%)} = 0.115 \text{ oil yield (l tonne}^{-1})$$

This means that, for this seam, the oil yield could have been assigned through TG measurements by multiplying the observed DTG pyrolysis peak area by 8.695 l tonne^{-1} wt.%$^{-1}$.

When the oil yield values for this seam are plotted versus depth at which each sample was taken, as shown in Fig. 13, one observes that the oil yield

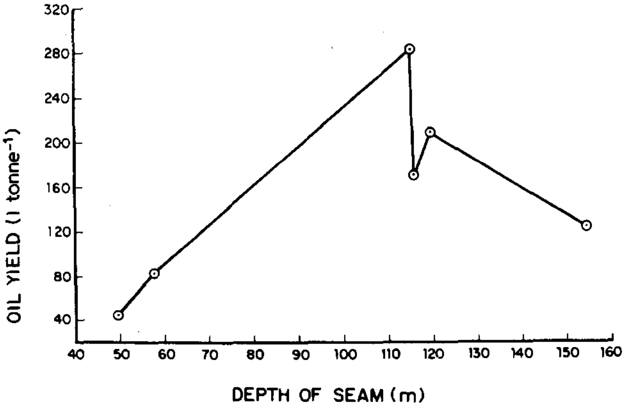

Fig. 13. Variation of oil yield with depth of seam.

increases with depth until a maximum is reached somewhere between 114.8 and 115.7 m. The oil yield then sharply declines. It was also observed in this study that the major DTG carbonate decomposition peak area varied inversely with the oil yield after reaching a seam depth of 60 m.

ACKNOWLEDGEMENTS

The author would like to express his appreciation to Robert F. Culmo for doing the elemental analyses presented in this work. Also to Dr. Allan Moritz, Prof. A.C. Cook, and Prof. Slade St. J. Warne for helpful discussions regarding the Australian oil shales.

REFERENCES

1 A. Cook, A. Hutton, A. Kantsler and S. Warne, Sci. Aust. 4 (1980) 6.
2 J.D. Baker, Symposium Papers: Synthetic fuels from oil shale, Inst. of Gas Tech., April 1980, p. 119.
3 C.S. Wen and T.G. Yen, Adv. Chem. Ser., 183 (1979) 343.
4 K. Rajeshwar, Thermochim. Acta, 45 (1981) 253.
5 K. Rajeshwar, Thermochim. Acta, 53 (1981) 121.
6 P.C. Uden, Proc. of the 10th NATAS Conf., Boston MA., Oct. 26–29, 1980, pp. 233–242.
7 A.J. Kraemer and H.M. Thorne, Oil shale operations in New South Wales Australia, U.S. Dept. of the Interior (Bur. of Mines) Rep. Invest., 1951, no. 4796.
8 K.E. Stanfield and I.C. Frost, U.S. Bur. of Mines Rep. Invest. U.S. 1946, No. 3977.
9 L. Goodfellow and M.T. Atwood, Q. Colo. Sch. Mines, 69 (2) (1974) 205.
10 C.M. Earnest, Thermochim. Acta, *in press*.
11 R.G. Mallon and R.L. Braun, Q. Colo. Sch. Mines, 71 (4) (1976) 309.
12 J.N. Smith et al., in J.H. Gary (Ed.), Proc. 11th Oil Shale Symp., Colorado School of Mines Press, 1978, pp. 100–112.
13 J.H. Campbell and A.K. Burnham, in J.H. Gary (Ed.), Proc. 11th Oil Shale Symp., Colorado School of Mines Press, 1978, pp. 242–259.
14 R.G. Mallon and R.L. Braun, in J.H. Gary (Ed.), Proc. 14th Oil Shale Symp., Colorado School of Mines Press, 1981, pp. 289–300.